The Cryosphere Discuss., https://doi.org/10.5194/tc-2017-158
Manuscript under review for journal The Cryosphere
Discussion started: 22 August 2017

The Cryosphere Discussions
Open Access

Change in Frozen Soils and Its Effect on Regional Hydrology in the Upper Heihe Basin, on the Northeastern Qinghai-Tibetan Plateau

Bing Gao[1], Dawen Yang[2]*, Yue Qin[2], Yuhan Wang[2], Hongyi Li[3], Yanlin Zhang[3], and Tingjun Zhang[4]

[1] School of Water Resources and Environment, China University of Geosciences, Beijing 100083, China

[2] State Key Laboratory of Hydroscience and Engineering, Department of Hydraulic Engineering, Tsinghua University, Beijing 100084, China

[3] Cold and Arid Regions Environmental and Engineering Research Institute, Chinese Academy of Sciences, Lanzhou, Gansu 730000, China

[4] Key Laboratory of West China's Environmental Systems (MOE), College of Earth and Environmental Sciences, Lanzhou University, Lanzhou, 730000, China

* *Correspondence to*: Dawen Yang (yangdw@tsinghua.edu.cn)

ABSTRACT:

Frozen ground has an important role in regional hydrological cycles and ecosystems, especially on the Qinghai-Tibetan Plateau, which is characterized by high elevation and a dry climate. This study modified a distributed physically based hydrological model and applied it to simulate the long-term (from 1971 to 2013) change of frozen ground and its effect on hydrology in the upper Heihe basin located in the northeastern Qinghai-Tibetan Plateau. The model was validated carefully against data obtained from multiple ground-based observations. Based on the model simulations, we analyzed the changes of frozen soils and their effects on the hydrology. The results showed that the permafrost area shrank by 9.5% (approximately 600 km^2), especially in areas with elevation between 3500 m and 3900 m. The maximum frozen depth of seasonally frozen ground decreased at a rate of approximately 5.2 cm/10yr, and the active layer depth over the permafrost increased by about 3.5 cm/10yr. Runoff increased significantly during cold seasons (November-March) due to the increase in liquid soil moisture caused by rising soil temperature. Areas where permafrost changed into seasonally frozen ground at high elevation showed especially large changes in runoff. Annual runoff increased due to increased precipitation, the base flow increased due to permafrost degradation, and the actual evapotranspiration increased significantly due to increased precipitation and soil warming. The groundwater storage showed an increasing trend, which indicated that the groundwater recharge was enhanced due to the degradation of permafrost in the study area.

KEYWORDS: permafrost; seasonally frozen ground; soil moisture; soil temperature;

The Cryosphere Discuss., https://doi.org/10.5194/tc-2017-158
Manuscript under review for journal The Cryosphere
Discussion started: 22 August 2017

The Cryosphere
Discussions
Open Access

runoff

1. Introduction

Global warming has led to significant changes in frozen soils, including both permafrost and seasonally frozen ground at high latitudes and high altitudes (Hinzman et al., 2013; Cheng and Wu, 2007). Changes in frozen soils can greatly affect the land-atmosphere interaction and the energy and water balances of the land surface (Subin et al., 2013; Schuur et al., 2015), altering soil moisture, water flow pathways and stream flow regime (Walvoord and Kurylyk, 2016). Understanding the changes in frozen soils and their impact on regional hydrology is important for water resources management and ecosystem protection in cold regions.

Previous studies based on either the experimental observations or long-term meteorological or hydrological observations have examined changes in frozen soils and their impacts on hydrology. Several studies reported that permafrost thawing might enhance base flow in the Arctic and the Subarctic (Walvoord and Striegl, 2007; Jacques and Sauchyn, 2009; Ye et al., 2009) and in northeast China (Liu et al., 2003; Duan et al., 2017). A few studies reported that permafrost thawing might reduce the river runoff, especially in the Qinghai-Tibetan Plateau (e.g. Qiu, 2012; Jin et al., 2009). Field experiments were usually carried out at small spatial scales over short periods, which lacked the regional pattern and long-term trends of the frozen soils, and the long-term meteorological and hydrological observations did not provide detailed data on soil freezing and thawing processes (McClelland et al., 2004; Liu et al., 2003; Niu et al., 2011). Therefore, the previous observation-based studies have not provided a sufficient understanding of the long-term changes in frozen soils and their impact on regional hydrology (Woo et al., 2008).

Hydrological models have been coupled with soil freezing-thawing schemes to simulate impacts of the changes in frozen soils on catchment hydrology. Several hydrological models (Rawlins et al., 2003; Chen et al., 2008) used simple freezing-thawing schemes, which could not simulate the vertical soil temperature profiles. The SiB2 model (Sellers et al., 1996), the modified VIC model (Cherkauer and Lettenmaier, 1999) and the CLM model (Oleson et al., 2010) simulate the vertical soil freezing-thawing processes, but they represent the hydrological processes especially the flow routing at the catchment scale, in overly simple ways. Subin et al. (2013) and Lawrence et al. (2015) used the CLM model to simulate the global change of permafrost. Cuo et al. (2015) used the VIC to simulate frozen soil degradation and its hydrological impacts at the plot scale in the headwater of the Yellow River. The GEOtop model (Endrizzi et al., 2014) simulates three-dimensional water flux and vertical heat transfer in soil, but it is difficult to apply to regional scales. Wang et al. (2010) and Zhang et al. (2013) incorporated frozen soil schemes in a distributed hydrological model and showed improved performance in a small mountainous catchment. More regional studies are necessary for better understanding of the frozen soil changes and their impacts on the regional hydrology and water resources.

The Qinghai-Tibetan Plateau is known as Asia's water tower, and runoff changes on the plateau have significant impacts on water security in the downstream regions (Walter et al., 2010), which have received an increasing amount of attention in recent years (Cuo et al., 2014). Hydrological processes on the Qinghai-Tibetan Plateau, which

The Cryosphere Discuss., https://doi.org/10.5194/tc-2017-158
Manuscript under review for journal The Cryosphere
Discussion started: 22 August 2017

is characterized by high elevation and cold climate are greatly influenced by cryospheric processes (Cheng and Jin, 2013; Cuo et al., 2014). In contrast with the Arctic and Subarctic, the permafrost thickness on the Qinghai-Tibetan Plateau is relatively thin and warm, and the frozen depth of the seasonally frozen soils is also relatively shallow. As a result, the frozen soils on the Qinghai-Tibetan Plateau are more sensitive to air the temperature rising (Yang et al., 2010), and the changes of frozen soils may have more significant impacts on regional hydrology.

An evident increase in the annual and seasonal air temperature has been observed in the Qinghai-Tibetan Plateau (Li et al., 2005; Liu and Chen, 2000; Zhao et al., 2004). Several studies have shown the changes of frozen soils based on long-term observations. For example, Cheng and Wu (2007) analyzed the borehole observations of soil temperature profiles on the Qinghai-Tibetan Plateau and found that the active layer thickness of frozen soils increased by 0.15-0.50 m during the period of 1996-2001. Zhao et al. (2004) found a decreasing trend of freezing depth in the seasonally frozen soils using observations at 50 stations. Several studies have analyzed the relationship between the change of frozen soils and river discharge using the observed data (Zhang et al., 2003; Jin et al., 2009; Niu et al., 2011). However, the spatio-temporal characteristics of the long-term change in frozen soils are not sufficiently clear. Having comprehensive experiments carried out by a major research plan, titled “Integrated research on the ecohydrological processes of the Heihe basin” funded by the National Natural Science Foundation of China (NSFC) (Cheng et al., 2014), a hydrological model coupling cryospheric processes and hydrological processes has been developed

The Cryosphere Discuss., https://doi.org/10.5194/tc-2017-158
Manuscript under review for journal The Cryosphere
Discussion started: 22 August 2017

(Gao et al., 2016). This provides a solid basis upon which to analyze the spatio-temporal changes in frozen soils and their impacts on the regional hydrology in the upper Heihe basin located on the northeastern Qinghai-Tibetan Plateau.

On the basis of the previous studies, this study aims to: (1) explore the spatial and temporal changes of frozen soils using a distributed hydrological model with comprehensive validation and (2) analyze the hydrological responses to the change of frozen soils during the past 40 years in the upper Heihe basin.

2. Study Area and Data

2.1 The Heihe River and the upper Heihe basin

The Heihe River is one of the major inland basins in northwestern China. As shown in Figure 1, the upper reaches of the Heihe River are located on the northeastern Qinghai-Tibetan Plateau at an elevation of 2200 to 5000 m with a drainage area of 10,009 km^2. The upper reaches provide the majority of the water supplied to the middle and lower reaches (Cheng et al., 2014). The annual precipitation in the upper Heihe basin ranges from 200 to 700 mm, and the annual mean air temperature ranges from -9 to 5℃. Permafrost dominates the high elevation region above 3700 m (Wang et al., 2013), and seasonal frozen ground covers other parts of the study area. Glaciers are found at an elevation above 4000 m, covering approximately 0.8% of the upper Heihe basin. There are two tributaries (East and West Tributaries) in the upper Heihe basin, on which two hydrological stations are located, namely, Qilian (on the east tributary) and Zhamashike (on the west tributary). The outlet of the upper Heihe basin has a hydrological station, namely, Yingluoxia (see Figure 1).

The Cryosphere Discuss., https://doi.org/10.5194/tc-2017-158
Manuscript under review for journal The Cryosphere
Discussion started: 22 August 2017

2.2 Data used in the study

(1) Forcing data of the hydrological model

The atmospheric forcing data used to drive the hydrological model include a 1-km gridded dataset of daily precipitation, air temperature, sunshine hours, wind speed and relative humidity. The gridded daily precipitation was interpolated from observations at meteorological stations (see Figure 1) provided by the China Meteorological Administration (CMA) using the method developed by Wang et al. (2017). The other atmospheric forcing data were interpolated by observations at meteorological stations using the inverse distance weighted method. The interpolation of air temperature considers the temperature gradient with elevation which was provided by the HiWATER experiment (Li et al., 2013).

The land surface data used to build the model include land use, topography, leaf area index, and soil parameters. The topography data were obtained from the SRTM dataset (Jarvis et al., 2008) with a spatial resolution of 90 m. The land use/cover data were provided by the Institute of Botany, Chinese Academy of Sciences (Zhou and Zheng, 2014). The leaf area index (LAI) data with 1-km resolution were developed by Fan (2014). The soil parameters were developed by Song et al. (2016); they include the saturated hydraulic conductivity, residual soil moisture content, saturated soil moisture content, soil sand matter content, soil clay matter content and soil organic matter content.

(2) Data used for model calibration and validation

This study uses the observed daily river discharge data from the Yingluoxia, Qilian and Zhamashike stations, the daily soil temperature of different depths from the Qilian station and the daily frozen depths from the Qilian and Yeniugou stations for model calibration and validation. Daily river discharge data were obtained from the Hydrology and Water Resources Bureau of Gansu Province. Daily soil temperature data collected at the Qilian station from January 1, 2004 to December 31, 2013, and daily frozen depth data collected at the Qilian and Yeniugou stations from January 1, 2002 to December 31, 2013 were provided by CMA.

To investigate the spatial distribution of permafrost, boreholes were drilled during the NSFC major research plan. Temperature observations from six boreholes, whose location are shown in Figure 1, were provided by Wang et al. (2013). The borehole depths are 100 m for T1, 69 m for T2, 50 m for T3, 90 m for T4, and 20 m for T5 and T7. Monthly actual evapotranspiration data with 1-km resolution during the period of 2002-2012 estimated based on remote sensing data (Wu et al., 2012; Wu, 2013) were used to evaluate the model-simulated evapotranspiration. We also used field observations of the hourly liquid soil moisture to validate the model simulation of soil moisture profiles. The HiWATER experiment (Li et al., 2013; Liu et al., 2011) provided the soil moisture data from January 1 to December 31, 2014 at the A'rou Sunny Slope station (100.52 E, 38.09 N).

3. Methodology

3.1 Brief introduction of the hydrological model

This study used a distributed eco-hydrological model GBEHM (geomorphology-based ecohydrological model), which was developed in an integrated research project under the major research plan "Integrated research on the ecohydrological process of the Heihe River Basin" (Yang et al., 2015; Gao et al., 2016) based on the geomorphology-based hydrological model (Yang et al., 1998 and 2002; Cong et al., 2009). As shown in Figure 2, the GBEHM used a 1-km grid system to discretize the study catchment, and the study catchment was divided into 251 sub-catchments. A sub-catchment was further divided into flow-intervals along its main stream. To capture the sub-grid topography, each 1-km grid was represented by a number of hillslopes with an average length and gradient, but different aspect, which were estimated from the 90-m DEM. The terrain properties of a hillslope include the slope length and gradient, slope aspect, soil type and vegetation type (Yang et al., 2015).

The hillslope is the basic unit for the hydrological simulation, upon which the water and heat transfers (both conduction and convection) in the vegetation canopy, snow/glacier, and soil layers are simulated. The canopy interception, radiation transfer in the canopy and the energy balance of the land surface are described using the methods used in SIB2 (Sellers et al., 1985, 1996). The surface runoff on the hillslope is solved using the kinematic wave equation. The groundwater aquifer is considered as individual storage units corresponding to each grid. Exchange between the groundwater and the river water is calculated using Darcy's law (Yang et al., 1998, 2002).

The model runs with a time step of 1 hour. Runoff generated from the grid is the lateral inflow into the river at the same flow interval in the corresponding sub-catchment. Flow routing in the river network is calculated using the kinematic wave equation following the sequence determined by the Horton-Strahler scheme (Strahler,

The Cryosphere Discuss., https://doi.org/10.5194/tc-2017-158
Manuscript under review for journal The Cryosphere
Discussion started: 22 August 2017

1957).

3.2 Simulation of cryospheric processes

The simulation of cryospheric processes in GBEHM includes glacier ablation, snow melt, and soil freezing and thawing.

(1) Glacier ablation

Glacier ablation is simulated using an energy balance model (Oerlemans, 2001) as:

$$Q_M = SW(1-\alpha) + LW_{in} - LW_{out} - Q_H - Q_L - Q_G + Q_R \tag{1}$$

where Q_M is the net energy absorbed by the surface of the glacier (W/m^2); SW is the incoming shortwave radiation (W/m^2); α is the surface albedo; LW_{in} is the incoming longwave radiation (W/m^2); LW_{out} is the outgoing longwave radiation (W/m^2); Q_H is the sensible heat flux (W/m^2); Q_L is the latent heat flux (W/m^2); Q_R is the energy from rainfall (W/m^2); and Q_G is the penetrating shortwave radiation (W/m^2). The surface albedo is calculated as (Oerlemans and Knap, 1998):

$$\alpha = \alpha_{snow} + (\alpha_{ice} - \alpha_{snow})e^{-h/d^*} \tag{2}$$

where α_{snow} is the albedo of snow on the glacier surface; α_{ice} is the albedo of the ice surface; h is the snow depth on the glacier surface (m); d^* is a parameter of the snow depth effect on the albedo (m).

The amount of melt water is calculated as (Oerlemans, 2001):

$$M = \frac{Q_M}{L_f} dt \tag{3}$$

where dt is the time step used in the model (s) and L_f is the latent heat of fusion (J/kg).

(2) Snow melt

A multi-layer snow cover model is used to describe the mass and energy balance of snow cover. The parametrization of snow is based on Jordan (1991), and each snow layer is described by two constituents, namely, ice and liquid water. For each snow layer, temperature is solved using an energy balance approach (Bartelt and Lehnin, 2002):

$$C_s \frac{\partial T_s}{\partial t} - L_f \frac{\partial \rho_i \theta_i}{\partial t} = \frac{\partial}{\partial z}(K_s \frac{\partial T}{\partial z}) + \frac{\partial I_R}{\partial z} + Q_R \tag{4}$$

where C_s is the heat capacity of snow (J·m^{-3}·K^{-1}); T_s is the temperature of the snow layer (K); ρ_i is the density of the ice (kg/m^3); θ_i is the volumetric ice content; K_s is the thermal conductivity of snow (W·m^{-1}·K^{-1}); L_f is the latent heat of ice fusion (J/kg) ; I_R is the radiation transferred into the snow layer (W/m^2) and Q_R is the energy brought by rainfall (W/m^2) which is only considered for the top snow layer. The solar radiation transfer in the snow layers and the snow albedo are simulated using the SNICAR model which is solved using the method developed by Toon et al. (1989). Eq. (4) is solved using an implicit centered finite difference method, and a Crank-Nicholson scheme is employed.

The mass balance of the snow layer is described as (Bartelt and Lehnin, 2002):

$$\frac{\partial \rho_i \theta_i}{\partial t} + M_{iv} + M_{il} = 0 \tag{5}$$

$$\frac{\partial \rho_l \theta_l}{\partial t} + \frac{\partial U_l}{\partial z} + M_{lv} - M_{il} = 0 \tag{6}$$

where ρ_l is the density of the liquid water (kg/m^3); θ_l is the volumetric liquid water content; U_l is the liquid water flux (kg·m^{-2}·s^{-1}); M_{iv} is the mass of ice that is changed into vapour within a time step (kg·m^{-3}·s^{-1}); M_{il} is the mass of ice that is changed into liquid water within a time step (kg·m^{-3}·s^{-1}); and M_{lv} is the mass of liquid water that is changed into vapour within a time step (kg·m^{-3}·s^{-1}). The liquid water flux of the snow layer is calculated as (Jordan, 1991):

The Cryosphere Discuss., https://doi.org/10.5194/tc-2017-158
Manuscript under review for journal The Cryosphere
Discussion started: 22 August 2017

$$U_l = -\frac{k}{\mu_l}\rho_l^2 g \tag{7}$$

where k is the hydraulic permeability (m^2), μ_l is dynamic viscosity of water at 0 ℃ (1.787×10^{-3} N s/m^2), ρ_l is the density of liquid water (kg/m^3) and g is gravitational acceleration (m/s^2). The water flux of the bottom snow layer is considered snowmelt runoff.

(3) Soil freezing and thawing

The energy balance of the soil layer is solved as (Flerchinger and Saxton, 1989):

$$C_s\frac{\partial T}{\partial t} - \rho_i L_f\frac{\partial \theta_i}{\partial t} - \frac{\partial}{\partial z}(\lambda_s\frac{\partial T}{\partial z}) + \rho_l c_l\frac{\partial q_l T}{\partial z} = 0 \tag{8}$$

where C_s is the volumetric soil heat capacity (J·m^{-3}·K^{-1}); T is the temperature (K) of the soil layers; z is the vertical depth of the soil (m); θ_i is the volumetric ice content; ρ_i is the density the ice (kg/m^3); λ_s is the thermal conductivity (W·m^{-1}·K^{-1}); ρ_l is the density of liquid water (kg/m^3); and c_l is the specific heat of liquid water (J·kg^{-1}·K^{-1}). In addition, q_l is the water flux between different soil layers (m/s) and is solved using the 1-D vertical Richards equation. The unsaturated soil hydraulic conductivity is calculated using the modified van Genuchten's equation (Wang et al., 2010) as:

$$K = f_{ice}K_{sat}(\frac{\theta_l-\theta_r}{\theta_s-\theta_r})^{1/2}[1-(1-(\frac{\theta_l-\theta_r}{\theta_s-\theta_r})^{-1/m})^m]^2 \tag{9}$$

where K is the unsaturated soil hydraulic conductivity (m/s); K_{sat} is the saturated soil hydraulic conductivity (m/s); θ_l is the volumetric liquid water content; θ_s is the saturated water content; θ_r is the residual water content; m is an empirical parameter in van Genuchten's equation and f_{ice} is an empirical hydraulic conductivity reduction factor which is calculated using soil temperature as (Wang et al., 2010):

$$f_{ice} = \exp[-10(T_f - T_{soil})], \quad 0.05 \le fice \le 1 \tag{10}$$

where T_f is 273.15 K and T_{soil} is the soil temperature.

Eq. (8) solves the soil temperature with the upper boundary condition as the heat flux into the top surface soil layer. When the ground is not covered by snow, the heat flux from the atmosphere into the top soil layer is expressed as (Oleson et al., 2010):

$$h = S_g + L_g - H_g - \lambda E_g + Q_R \tag{11}$$

where h is the upper boundary heat flux into the soil layer (W m^{-2}); S_g is the solar radiation absorbed by the top soil layer (W m^{-2}); L_g is the net long wave radiation absorbed by the ground (W m^{-2}), H_g is the sensible heat flux from the ground (W m^{-2}); λE_g is the latent heat flux from the ground (W m^{-2}); and Q_R is the energy brought by rainfall (W/m^2). When the ground is covered by snow, the heat flux into the top soil layer is calculated as:

$$h = I_p + G \tag{12}$$

where I_p is the radiation that penetrates the snow cover, and G is the heat conduction from the bottom snow layer to the top soil layer. Eq (8) is solved using a finite difference scheme with an hourly time step which is similar with the solutions of Eq (4).

To simulate the permafrost we consider an underground depth of 50 m and assume the bottom boundary condition as zero heat flux exchange. The vertical soil column is divided into 39 layers in the model (see Figure 2). The topsoil of 1.7 m is subdivided into 9 layers. The first layer is 5 cm, and the soil layer thickness increases with depth linearly from 5 cm to 30 cm up to the depths of 0.8 m and later decreases linearly with depth to 10 cm up to the depths of 1.7 m. There are 12 soil layers from 1.7 m to 3.0 m with a constant thickness of 10 cm. From the depth of 3 m to 50 m, there are 18 layers with thickness increasing exponentially from 10 cm to 12 m. The liquid soil moisture, ice content, and soil temperature of each layer is calculated at each time step. The soil heat capacity and soil thermal conductivity are estimated using the method developed by Farouki (1981).

3.3 Model calibration

We assume that there is a linear relationship between soil temperature and elevation at the same depth below surface. The relationship between soil temperature at a specific depth and elevation is estimated from the observed soil temperature at 6 boreholes (see Figure 1). For spin up run, the initial soil temperatures at different depths for all grids of the whole study area were interpolated from the borehole observations using this relationship. Next, the model had a 500 year spin up run to specify the initial values of the hydrological variables (e.g., soil moisture, soil temperature, soil ice content, and groundwater table) by repeating the atmospheric forcing data from 1961 to 1970.

The period of 2002 to 2006 was used for model calibration and the period of 2008 to 2012 was for model validation. The daily soil temperature at the Qilian station and the frozen depths at the Qilian and Yeniugou stations were used to calibrate the soil reflectance according to vegetation type. The other parameters such as groundwater hydraulic conductivity were calibrated according to the baseflow discharge in the winter season. We calibrated the surface retention capacity and surface roughness to match the observed flood peaks, and calibrated the leaf reflectance, leaf transmittance and maximum Rubsico capacity of the top leaf based on the remote sensing evapotranspiration data. Table 1 shows the major parameters used in the model.

4. Results

4.1 Validation of the hydrological model

We carried out a comprehensive validation of the GBEHM model using the soil temperature profiles observed at six boreholes, long-term observations of the soil temperature and frozen depths at two CMA stations, soil moisture observations at one HiWATER station, long-term observations of streamflow at three hydrological stations and monthly actual evapotranspiration estimated from remote sensing data.

Figure 3 shows the comparison of the model-simulated and observed soil temperature profiles at six boreholes. The model was generally accurate in capturing the vertical distribution of the soil temperature at T1, T2, T3 and T4 in the permafrost area, but overestimations were produced above 20 m depth for T1 and T3. Good agreement between the simulated and observed soil temperature profiles below the depth of 20 m implies that the temperature in the deep soil is stable, which is confirmed by the comparison of temperature profiles in different years as shown in Figure S1 in the supplemental file. Figure S1 also illustrates that temperature above 20 m shows significant increasing trends in the past 40 years. The errors in simulating the vertical temperature profile near the surface might be caused by simplification of the 3-D topography. At T5 located in seasonally frozen ground, the simulated soil temperature profile did not agree well with that observed at depth of 4-20 m. This error might also be related to the heterogeneity of soil properties, especially the thermal conductivity and heat capacity since no such information is available. The model simulation agrees well with the borehole observation at T7, which is located at the transition zone from permafrost to seasonally frozen ground. This indicates that the model can identify the boundary of the permafrost and the seasonally frozen ground.

We also validated model simulation of the freezing/thawing cycles based on long-term observations of soil temperature and frozen depth. Figure 4 compares the simulated soil temperature with the observed temperature at the Qilian station, which is located in the seasonally frozen ground (observed daily soil temperature data are available from 2004 on). Generally, the model simulations accurately captured the seasonal changes in soil temperature profile. Validation of the soil temperature at different depths (5 cm, 10 cm, 20 cm, 40 cm, 80 cm, 160 cm, and 320 cm) showed that the root mean square error (RMSE) decreases with increasing depth. The RMSE were approximately 2.5℃ for the top three depths (5 cm, 10 cm and 20 cm). The RMSE for depths of 40 cm and 80 cm were 1.7℃ and 1.5℃, respectively, and the RMSE was 0.9℃ at a depth of 3.2 m. We compared the model-simulated daily frozen depth with in situ observations at the Qilian and Yeniugou Stations from 2002 to 2014, as shown in Figure 5. The model reproduced well the daily variations in frozen depth although the depth was underestimated by approximately 50 cm at the Yeniugou station. In general, the validation of soil temperature and frozen depth indicates that the model captured well the freezing and thawing processes in the upper Heihe basin.

The observed hourly liquid soil moisture at the A’rou Sunny Slope station was used for an additional independent validation. Figure 6 shows the comparison between the simulated and observed liquid soil moisture at different depths from January 1 to December 31 in 2014. By comparing with the observed liquid soil moisture, we can see that the model simulation is reasonable.

Figure 7 compares the model simulated and the observed daily streamflow discharge at the Yingluoxia, Qilian and Zhamashike station. The model simulation agreed well with the observations. The model simulation captured the flood peaks and the magnitude of base flow in both of the calibration and validation periods. In the calibration period, the Nash-Sutcliffe efficiency (NSE) coefficients were 0.64, 0.65 and 0.70 for the Yingluoxia, Qilian and Zhamashike stations, respectively; in the validation period, the NSE values were 0.65, 0.60, and 0.75, respectively. The relative error (RE) was within 10% for both the calibration and validation periods (see Figure 7). Figure 8 shows the comparison of the model-simulated monthly actual evaporation and remote sensing-based evaporation data for the entire calibration and validation periods. The GBEHM simulation showed similar temporal variations in actual evapotranspiration compared with the remote sensing based estimation, and the RMSE of the simulated monthly evapotranspiration was 8.0 mm in the calibration period and 6.3 mm in the validation period.

The model simulated river discharges with and without the frozen soil scheme were compared. Table S1 in the supplement material shows that model with the frozen soil scheme achieves better simulation of the daily hydrograph than the model without the frozen soil scheme. Figure S2 in the supplement material shows that the model without the frozen soil scheme overestimated the river discharge in the freezing season and

The Cryosphere Discuss., https://doi.org/10.5194/tc-2017-158
Manuscript under review for journal The Cryosphere
Discussion started: 22 August 2017

underestimated flood peaks in the warming season.

4.2 Long-term changes in frozen soils

In the upper Heihe basin, the ground surface starts freezing in November and thawing initiates in April (Wang et al., 2015a). From November to March, the ground surface temperature is below 0℃ in both the permafrost and seasonally frozen ground regions, and precipitation mainly falls in the period from April to October. Therefore, a year is subdivided into two seasons, i.e., the freezing season (November to March) and the thawing season (April to October) to investigate the changes in frozen soils and their hydrological impact. Increasing precipitation and air temperature in the study area in both seasons in the past 50 years was reported in a previous study (Wang et al., 2015b).

Figure 9 shows the changes in the basin-averaged soil temperature in the freezing and thawing seasons. The soil temperature increased in all seasons, especially in the past 30 years. The increasing trend of soil temperature was larger in the freezing season than in the thawing season. In the freezing season (Figure 9(a)), the top layer soil temperature was lower than the deep layer soil temperature. The linear trend of the top layer (0-0.5 m) soil temperature was 0.48℃/10yr and the trend of the deep layer (2.5-3 m) soil temperature was 0.34℃/10yr. The soil temperature in the deep layer (2.5-3 m) changed from -1.1℃ in the 1970s to approximately 0℃ in the most recent decade. In the thawing season (see Figure 9(b)), the increasing trend of the top layer (0-0.5 m) soil temperature (0.29℃/10yr) was greater than the trend of the deep layer (2.5-3 m) soil temperature (0.21℃/10yr). The warming trend is larger in shallow soils and this is because the surface heat flux is impeded by the thermal inertia as it penetrates to greater

The Cryosphere Discuss., https://doi.org/10.5194/tc-2017-158
Manuscript under review for journal The Cryosphere
Discussion started: 22 August 2017

depths.

Permafrost is defined as ground with a temperature at or below 0℃ for at least two consecutive years (Woo, 2012). This study differentiated permafrost from seasonally frozen ground based on the simulated vertical soil temperature profile in each grid. For each year in each grid, the frozen ground condition was determined by searching the soil temperature profile within a four-year window from the previous three years to the current year. Figure 10 shows the change in permafrost area during 1971-2013. As shown in Figure 10(a), the permafrost areas decreased by approximately 9.5% (from 6445 km^2 in the 1970s to 5831 km^2 in the 2000s), indicating evident degradation of the permafrost in the upper Heihe basin in the past 40 years.

Figure 10 (b) shows the changes in the basin-averaged maximum frozen depth for the seasonally frozen ground areas and active layer thickness over the permafrost areas. The basin-averaged annual maximum frozen depth showed a significant decreasing trend (5.2 cm/10yr). In addition, the maximum frozen depth had a significantly negative correlation with the annual mean air temperature (r = -0.73). In contrast, an increasing trend of active layer thickness in the permafrost regions was observed (3.5 cm/10yr), which had a significantly positive correlation with the annual mean air temperature.

Figure 11 shows the frozen soil distributions in the period of 1971 to 1980 and in the period of 2001 to 2010. Comparing the frozen soil distributions of the two periods, major changes in frozen soils were observed on the sunny slopes at elevations between 3500 and 3700 m, especially in the west tributary, where large areas of permafrost changed into seasonally frozen ground.

Figure 12 shows the monthly mean soil temperature over the areas with elevation between 3300 and 3500 m and over areas with elevation between 3500 and 3700 m in the upper Heihe basin. In the areas with elevation between 3300 and 3500 m located in the seasonally frozen ground region, as shown in Figure 12(a), the frozen depth decreased and the soil temperature in the deep layer (with depth greater than 2 m) increased. Figure 12(b) shows that the increase in soil temperature was larger in the area with higher elevation (3500-3700 m). This figure shows that the thickness of the permafrost layer decreased as soil temperature increased, and the permafrost changed into seasonally frozen ground after 2000.

4.3 Changes in the water balance and runoff

Table 2 shows the decadal changes in the annual water balance from 1971 to 2010 based on the model simulation. The annual precipitation, annual runoff and annual runoff ratio had the same decadal variation; however the annual evapotranspiration maintained an increasing trend since the 1970s which was consistent with the rising air temperature and soil warming. Although the actual evapotranspiration increased, the runoff ratio remained stable during the 4 decades because of the increased precipitation.

The changes in runoff (both simulated and observed) in different seasons are shown in Figure 13 and Table 2. The model-simulated and observed runoff both showed a significant increasing trend in the freezing season and in the thawing season. This indicates that the model simulation accurately reproduced the observed long-term changes. In the freezing season, since there was no glacier melt and snow melt (see Table 2), runoff was mainly the subsurface flow (groundwater flow and lateral flow

The Cryosphere Discuss., https://doi.org/10.5194/tc-2017-158
Manuscript under review for journal The Cryosphere
Discussion started: 22 August 2017

from the unsaturated zone). In the thawing season, as shown in Table 2, snowmelt runoff contributed approximately 16% of the total runoff and glacier runoff contributed only a small fraction of total runoff (approximately 2.4%). Therefore, rainfall runoff was the major component of total runoff in the thawing season, and the runoff increase in the thawing season was mainly due to increased rainfall. As shown in Figure 13, the actual evapotranspiration increased significantly in both seasons due to increased precipitation and soil warming. The increasing trend of the actual evapotranspiration was higher in the thawing season than in the freezing season.

Figure 14 shows the changes in the basin-averaged annual water storage in the top 0-3 m layer and the groundwater storage. The annual liquid water storage of the top 0-3 m showed a significant increasing trend especially in the most recent 3 decades. This long-term change in liquid water storage was similar to the runoff change in the freezing season, as shown in Figure 13 (a), with a correlation coefficient of 0.80. The annual ice water storage in the top 0-3 m soil showed significant decreasing trend due to frozen soils changes. Annual groundwater storage showed a significantly increasing trend especially in the most recent 3 decades, which indicates that the groundwater recharge increases with the frozen soil degradation.

5. Discussion

5.1 Impact of frozen soil changes on the soil moisture and runoff

Based on the model simulated daily soil moisture, long-term changes of the spatially averaged liquid soil moistures in the region with elevation between 3300 and 3500 m (covered by the seasonally frozen ground) and in the region with elevation between

3500 and 3700 m (where the permafrost changed into seasonally frozen ground) are shown in Figure S3 in the supplement material. In the seasonally frozen ground with elevation of 3300-3500 m, by comparing with the soil temperature shown in Figure 12 (a), we can see that the liquid soil moisture increase was mainly caused by the decrease in the frozen depth. The liquid soil moisture in the deep soil layer increased significantly since the 1990s in the area with elevation of 3500-3700 m where the permafrost changed to seasonally frozen ground. Compared with the soil temperature change shown in Figure 12 (b), the liquid soil moisture increases in this region were primarily caused by the change of permafrost to seasonally frozen ground, indicating that the frozen soil degradation caused a significant increase in liquid soil moisture in both the freezing and thawing seasons.

In the freezing season, since the surface ground is frozen, runoff is mainly subsurface flow coming from the seasonally frozen ground. Runoff has the highest correlation (r=0.82) with the liquid soil moisture in the freezing season, which indicates that the frozen soils change was the major cause of the increased liquid soil moisture, resulting in increased runoff in the freezing season. During the past 40 years, parts of the permafrost changed into seasonally frozen ground, and the thickness of the seasonally frozen ground decreased, which led to increased liquid soil moisture in the deep layers during the freezing season. The increase in liquid soil moisture also increased the hydraulic conductivity which enhanced the subsurface flow.

In the thawing season from April to October, the thickness of the seasonally frozen ground rapidly decreased to zero and the thaw depth of permafrost reached the maximum. Runoff in the thawing season was mainly rainfall runoff, as shown in Table 2. The increased runoff mainly came from increased precipitation in the thawing season.

Figure 15 shows the changes in areal mean runoff along the elevation for different seasons. There was a large difference in runoff variation with the elevation during the different seasons. In the freezing season, the runoff change from the 1970s to the 2000s in the areas of seasonally frozen ground (mainly located below 3500 m, see Figure 11) was relatively small. The areas with elevations of 3500 to 3900 m showed larger changes in runoff. This is due to the shift from permafrost to seasonally frozen ground in some areas in the elevation range of 3500 to 3900 m, as simulated by the model, particularly for the sunny hillslopes (see Figure 11). This finding illustrates that a change from the permafrost to the seasonally frozen ground has a larger impact on the runoff than a change in frozen depth in the seasonally frozen ground. In the thawing season, runoff increased with elevation due to the increase in precipitation with increasing elevation, and the runoff increase was mainly determined by increased precipitation (Gao et al., 2016). Precipitation in the region with elevation below 3100 m was low, but air temperature was high. Runoff in this region decreased during 2001-2010 compared to 1971-1980 because of higher evapotranspiration.

5.2 Comparison with the previous similar studies

In this study, the model simulation showed that changes in frozen soils led to increased freezing season runoff and base flow in the upper Heihe basin. This result is consistent with previous findings based on the trend analysis of streamflow observations in high latitude regions (Walvoord and Striegl, 2007; Jacques and Sauchyn, 2009; Ye et al., 2009) and in northeast China (Liu et al., 2003). However, those studies did not consider spatial variability. This study found that the impact of the change in frozen soils on runoff had regional characteristics. In the upper Heihe basin (see Figure 15), a change in frozen soils led to increased runoff at higher elevations but led to decreased runoff at lower elevations during the freezing season. This implies that change of the freezing season runoff was controlled by the permafrost degradation in the higher elevation region but by the evaporation increase in the lower elevation region due to the air temperature rising. However, runoff at the basin scale mainly came from the higher elevation regions.

This study also showed that the change in frozen soils increased the soil moisture in the upper Heihe basin, which is consistent with the finding of Subin et al. (2013) using the CLM model simulation in northern latitude permafrost regions, and the findings of Cuo et al. (2015) using VIC model simulation at 13 sites on the Tibetan Plateau. However, Lawrence et al. (2015) found that permafrost thawing caused soil moisture drying based on CLM model simulations for the global permafrost region. This might be related to the uncertainties in the soil water parameters and the high spatial heterogeneity of soil properties, which are difficult to consider in a global-scale model. Subin et al. (2013) and Lawrence et al. (2015) modelled the soil moisture changes in the active layer of permafrost in large areas with coarse spatial resolution. This study revealed the spatio-temporal variability of soil moisture with high spatial resolution and analyzed the correlations with the change in frozen soils.

Wu and Zhang (2010) focused on the changes in the active layer thickness at 10 sites

The Cryosphere Discuss., https://doi.org/10.5194/tc-2017-158
Manuscript under review for journal The Cryosphere
Discussion started: 22 August 2017

in the permafrost region on the Tibetan Plateau and found a significant increasing trend during the period of 1995-2007, which is consistent with the result of this study. Jin et al. (2009) found decreased soil moisture and runoff due to the permafrost degradation based on observations at the plot scale in the source areas in the Yellow River basin. This result is different from the present study, possibly due to the difference of hydrogeological structure and the soil hydraulic parameters in the source area of the Yellow River from those in the upper Heihe basin. Wang et al. (2015a) focused on the change in the seasonally frozen ground in the Heihe River basin based on plot observations, and the increasing trend of the maximum frozen depth was estimated as 4.0 cm/10yr during 1972-2006, which is consistent with the GBEHM model simulation in this study. The increase in groundwater storage illustrated in this study is also consistent with the finding of Cao et al. (2012) based on the GRACE data which showed that groundwater storage increased during the period of 2003~2008 in the upper Heihe basin.

5.3 Uncertainty in simulation of the frozen soils

Estimation of the change in permafrost area is a great challenge due to such complex factors as climatology, vegetation, and geology. Different methods produce large differences in their estimation results. Jorgenson et al. (2006) found a 4.4% decrease in the area of permafrost in Arctic Alaska from 1982 to 2001 based on analyses of aerial photo. Wu et al. (2005) reported that the permafrost area decreased by 12% from 1975 to 2002 in the Xidatan basin, Qinghai-Tibetan Plateau based on a ground penetration radar survey. Jin et al. (2006) found an area reduction of 35.6% in island permafrost in

Liangdaohe, which is located at the southern Qinghai–Tibet Highway, from 1975 to 1996. Chasmer et al. (2010) found a 30% reduction of the discontinuous permafrost area in the Northwest Territories, Canada from 1947 to 2008 based on remote sensing. Compared with the borehole observations by Wang et al. (2013) shown in Figure 2, this model slightly overestimated the soil temperature in permafrost areas, which might lead to overestimation of the rate of permafrost area reduction.

There were two major uncertainties in the frozen soils simulation which may lead to overestimation: uncertainty in the land surface energy balance simulation and uncertainty in the simulation of the soil heat-water transfer processes (Wu et al., 2016). Uncertainty in the land surface energy balance simulation might result from the estimations of radiation and surface albedo due to the complex topography, vegetation cover and soil moisture distribution, which may introduce uncertainties in the estimated ground temperature and thermal heat flux into the deep layers. The uncertainty in simulation of soil heat-water transfer processes might result from the soil water and heat parameters and the bottom boundary condition of heat flux. Permafrost degradation is closely related to the thermal properties of rocks and soils, geothermal flow and initial soil temperature and soil ice conditions. The lack of observed initial condition data could also cause uncertainty in the permafrost change estimation. For discontinuous permafrost, lateral heat flux may increase the thawing rate (Kurylyk et al., 2016; Sjöberg et al., 2016) and this effect is not considered in the present study. This may lead to underestimation of thawing rates of discontinuous permafrost, especially in spring. In addition, uncertainties from input data, particularly the solar

The Cryosphere Discuss., https://doi.org/10.5194/tc-2017-158
Manuscript under review for journal The Cryosphere
Discussion started: 22 August 2017

radiation which is estimated using interpolated sunshine hour data from limited observational stations and precipitation which is also interpolated by observations at these stations, may also influence the results of the model simulation.

6. Conclusions

A distributed hydrological model coupled with cryospheric processes was carefully validated in the upper Heihe River basin using available observations of soil moisture, soil temperature, frozen depth, actual evaporation and streamflow discharge. Based on the model simulations from 1971 to 2013 in the upper Heihe River, the long-term changes in frozen soils were investigated, and the effect of the frozen soils change on hydrological processes were explored. Based on these analyses, the following conclusions can be drawn:

(1) The model simulation suggests that 9.5% of permafrost areas degraded into seasonally frozen grounds in the upper Heihe River basin during the period of 1971 to 2013, which predominantly occurred at the elevations between 3500 m and 3900 m. The decreasing trend of annual maximum frozen depth is estimated to be 5.2 cm/10yr for the seasonally frozen grounds, which is consistent with previous observation-based studies at plot scale. The increasing trend of active layer thickness is estimated to be 3.5 cm/10yr in the permafrost regions.

(2) Model simulated trends in runoff agree with the observed trends. In the freezing season (November-March), based on the model simulation, runoff was mainly sourced by subsurface flow which increased significantly in the higher elevation regions where significant frozen soil changes occurred. This finding implies that runoff increase in the

freezing season is primarily caused by frozen soil changes (permafrost degradation and decrease of the seasonally frozen depth). In the thawing season (April-October), model simulation indicates that runoff mainly came from rainfall and showed an increasing trend at the higher elevations, which can be explained by the increased precipitation. In both the freezing and thawing seasons, model simulated runoff decreased in the lower elevation region, which can be explained by increased evaporation due to the rising air temperature.

(3) Model simulated changes in soil moisture and soil temperature indicates that annual storage of the liquid water increased especially in the most recent three decades, due to the change in frozen soils. Annual ice water storage in the top 0-3 m of soil showed a significant decreasing trend due to soil warming. Model simulated annual groundwater storage had an increasing trend, which is consistent with the changes observed by the GRACE satellite. This indicated that groundwater recharge in the upper Heihe basin was enhanced in recent decades.

(4) Model simulation indicated that regions where the permafrost changed into the seasonally frozen ground had larger changes in runoff and soil moisture than the areas covered by seasonally frozen ground.

For a better understanding of changes in frozen soils and their impact on ecohydrology, the interactions among the soil freezing-thawing processes, vegetation dynamics and hydrological processes need to be investigated in future studies. There are uncertainties in simulations of the frozen soils and the hydrological processes that might be related to the soil properties, the high spatial heterogeneity, and the parameterization of the lower soil boundary conditions, all of which warrant further investigation in the future.

Acknowledgements: This research was supported by the major plan of "Integrated Research on the Ecohydrological Processes of the Heihe Basin" (Project Nos. 91225302 and 91425303) funded by the National Natural Science Foundation of China (NSFC). The authors would like to thank the editor for their constructive comments, which greatly improved the manuscript.

References

Bartelt P. and M. Lehning: A physical snowpack model for the swiss avalanche warning: Part Ⅰ: numerical model, Cold Regions Sci. and Tech., 35(3), 123-145, doi: 10.1016/S0165-232X(02)00074-5, 2002.

Chasmer L., C. Hopkinson and W. Quinton: Quantifying errors in discontinuous permafrost plateau change from optical data, Northwest Territories, Canada: 1947–2008, Canadian Journal of Remote Sensing, 36:sup2, S211-S223, doi: 10.5589/m10-058, 2010.

Cao Y., Nan Z. and Hu X.: Estimating groundwater storage changes in the Heihe river basin using GRACE, in: IEEE International Geoscience and Remote Sensing Symposium (IGARSS), Munich, Germany, 22–27 July 2012, 798-801, 2012.

Chen, R., Lu, S., Kang, E., Ji, X., Zhang, Z., Yang, Y., Qing, W.: A distributed water-heat coupled model for mountainous watershed of an inland river basin of Northwest China (I) model structure and equations, Environ. Geol., 53, 1299-1309, doi: 10.1007/s00254-007-0738-2,2008.

The Cryosphere Discuss., https://doi.org/10.5194/tc-2017-158
Manuscript under review for journal The Cryosphere
Discussion started: 22 August 2017

Cheng, G. and Jin, H.: Permafrost and groundwater on the Qinghai-Tibet Plateau and in northeast China, Hydrogeol. J., 21, 5-23, doi: 10.1007/s10040-012-0927-2, 2013.

Cheng, G., Li, X., Zhao, W., Xu, Z., Feng, Q., Xiao, S., Xiao, H.: Integrated study of the water-ecosystem-economy in the Heihe River Basin. Nat. Sci. Rev., 1(3), 413-428, doi: 10.1093/nsr/nwu017, 2014.

Cheng, G., and Wu T.: Responses of permafrost to climate change and their environmental significance, Qinghai-Tibet Plateau, J. Geophys. Res., 112, F02S03, doi:10.1029/2006JF000631, 2007.

Cherkauer, K. A., and D. P. Lettenmaier: Hydrologic effects of frozen soils in the upper Mississippi River basin, J. Geophys. Res., 104, 19,599-19,610, doi: 10.1029/1999JD900337, 1999.

Cong Z T, Yang D W, Gao B, et al.: Hydrological trend analysis in the Yellow River basin using a distributed hydrological model, Water Resour Res, 45: W00A13, doi: 10.1029/2008WR006852, 2009

Cuo, L., Y. Zhang, F. Zhu, and L. Liang.: Characteristics and changes of streamflow on the Tibetan Plateau: A review, J. Hydrol.: Reg. Stud., 2, 49-68, doi: 10.1016/j.ejrh.2014.08.004, 2014.

Cuo, L., Y. Zhang, T. J. Bohn, L. Zhao, J. Li, Q. Liu, and B. Zhou: Frozen soil degradation and its effects on surface hydrology in the northern Tibetan Plateau, J. Geophys. Res. Atmos., 120, doi:10.1002/2015JD023193, 2015.

Duan L., Man X., Kurylyk B. L. and Cai T.: Increasing winter baseflow in response to permafrost thaw and precipitation regime shifts in northeastern China, Water, 9(1), 25, doi:10.3390/w9010025, 2017.

Endrizzi S, Gruber S, Dall'Amico M, and R. Rigon: GEOtop 2.0: simulating the combined energy and water balance at and below the land surface accounting for soil freezing, snow cover and terrain effects, Geosci. Model Dev., 7: 2831-2857, doi:10.5194/gmd-7-2831-2014, 2014.

Fan, W.: Heihe 1km LAI production, Heihe Plan Science Data Center at Lanzhou, doi:10.3972/heihe.090.2014.db, 2014.

Farouki, O.T.: The thermal properties of soils in cold regions, Cold Regions Sci.and Tech., 5, 67-75, doi: 10.1016/0165-232X(81)90041-0, 1981.

Flerchinger G., Saxton K.: Simultaneous heat and water model of a freezing snow-residue-soil system I. Theory and development, Trans. ASAE, 32, 565-571, doi: 10.13031/2013.31040, 1989.

Gao B., Qin Y., Wang YH, Yang DW, and Zheng YR: Modeling Ecohydrological Processes and Spatial Patterns in the Upper Heihe Basin in China, Forests, 7(1),10, doi:10.3390/f7010010, 2016.

Hinzman, L.D., C.J. Deal, A.D. McGuire, S.H. Mernild, I.V. Polyakov, and J.E. Walsh: Trajectory of the Arctic as an integrated system, Ecol. Appl., 23(8),1837-1868, doi:10.1890/11-1498.1, 2013.

Jacques St., J.-M., and Sauchyn D. J.: Increasing winter baseflow and mean annual streamflow from possible permafrost thawing in the Northwest Territories, Canada, Geophys. Res. Lett., 36, L01401, doi:10.1029/2008GL035822, 2009.

Jarvis, A., Reuter, H.I., Nelson, A., Guevara, E.: Hole-filled seamless SRTM data, Version 4, International Centre for Tropical Agriculture (CIAT), 2008.

Jin, H., He, R., Cheng, G., Wu, Q., Wang, S., Lu, L. and Chang X.: Changes in frozen ground in the Source Area of the Yellow River on the Qinghai–Tibet Plateau, China, and their eco-environmental impacts, Environ. Res. Lett., 4(4), 045206, doi:10.1088/1748-9326/4/4/045206, 2009.

Jin, H.J., Zhao, L., Wang, S.L., Jin, R.: Thermal regimes and degradation modes of permafrost along the Qinghai–Tibet Highway, Science in China D: Earth Sciences, 49 (11), 1170-1183, 2006.

Jordan R.: A one-dimensional temperature model for a snow cover, Technical Documentation for SNTHERM.89, Cold Regions Research and Engineering Lab, Hanover NH, 49 pp., 1991.

The Cryosphere Discuss., https://doi.org/10.5194/tc-2017-158
Manuscript under review for journal The Cryosphere
Discussion started: 22 August 2017

The Cryosphere Discussions
Open Access EGU

Jorgenson, M. T., Y. L. Shur, and E. R. Pullman: Abrupt increase in permafrost degradation in Arctic Alaska, Geophys. Res. Lett., 33, L02503, doi:10.1029/2005GL024960, 2006.

Kurylyk, B. L., M. Hayashi, W. L. Quinton, J. M. McKenzie, and C. I. Voss: Influence of vertical and lateral heat transfer on permafrost thaw, peatland landscape transition, and groundwater flow, Water Resour. Res., 52, 1286-1305, doi:10.1002/2015WR018057, 2016.

Lawrence, D.M., C.D. Koven, S.C. Swenson, W.J. Riley, and A.G. Slater: Permafrost thaw and resulting soil moisture changes regulate projected high-latitude CO_2 and CH_4 emissions, Environ. Res. Lett., 10, doi:10.1088/1748-9326/10/9/094011, 2015.

Li, D.L., Zhong, H.L., Wu, Q.B., Zhang, Y.J., Hou, Y.L., Tang, M.C.: Analyses on changes of surface temperature over Qinghai–Xizang Plateau, Plateau Meteorology, 24, 291-298, 2005 (in Chinese).

Li, X., Cheng, G.D., Liu, S.M., Xiao, Q., Ma, M.G., Jin, R., Che, T., Liu, Q.H., Wang, W.Z., Qi, Y., Wen, J.G., Li, H.Y., Zhu, G.F., Guo, J.W., Ran, Y.H., Wang, S.G., Zhu, Z.L., Zhou, J., Hu, X.L., Xu, Z.W.: Heihe Watershed Allied Telemetry Experimental Research (HiWATER): Scientific Objectives and Experimental Design, B. Am. Meteorol. Soc., 94(8), 1145-1160, doi: 10.1175/BAMS-D-12-00154.1, 2013.

Liu, X. and Chen, B.: Climate warming in the Tibetan Plateau during recent decades, Int. J. Climatol., 20(1), 1729-1742, doi: 10.1002/1097-0088(20001130)20:14<1729::AID-JOC556>3.0.CO;2-, 2000.

Liu, S., Xu Z., Wang W., Bai J., Jia Z., Zhu M., and Wang J.: A comparison of eddy-covariance and large aperture scintillometer measurements with respect to the energy balance closure problem, Hydrol. Earth Syst. Sc., 15(4), 1291-1306, doi:10.5194/hess-15-1291-2011, 2011.

Liu J., N. Hayakawab, Lu M., Dong S., and Yuan J.: Hydrological and geocryological response of winter streamflow to climate warming in Northeast China, Cold Regions Sci.and Tech., 37,15-24, doi:

10.1016/S0165-232X(03)00012-0, 2003.

Wu T., Li S., Cheng G. and N Z.: Using ground-penetrating radar to detect permafrost degradation in the northern limit of permafrost on the Tibetan Plateau, Cold Regions Sci.and Tech., 41, 211-219, 2005, doi:10.1016/j.coldregions.2004.10.006.

Niu L., Ye B., Li J., and Sheng Y.: Effect of permafrost degradation on hydrological processes in typical basins with various permafrost coverage in Western China, China Earth Sci., 54(4), 615-624, doi: 10.1007/s11430-010-4073-1, 2011.

Oerlemans, J. and Knap, W.H.: A 1 year record of global radiation and albedo in the ablation zone of Morteratschgletscher, Switzerland, J. Glaciol., 44, 231-238, doi: 10.3198/1998JoG44-147-231-238, 1998.

Oerlemans, J.: Glaciers and Climate Change, Lisse: Swets & Zeitlinger, 2001.

Oleson, K.W., Lawrence, D.M., Bonan, G.B., Flanner, M.G., Kluzek, E., Lawrence, P.J., Levis, S., Swenson, S.C., Thornton, P.E., Dai, A., Decker, M., Dickinson, R., Feddema, J., Heald, C.L., Hoffman, F., Lamarque, J., Mahowald, N., Niu, G., Qian, T., Randerson, J., Running, S., Sakaguchi, K., Slater, A., Stöckli, R., Wang, A., Yang, Z., Zeng, X., Zeng, X.: Technical Description of version 4.0 of the Community Land Model (CLM), NCAR Technical Note NCAR/TN-47+STR, National Center for Atmospheric Research, Boulder, CO, 257 pp., 2010.

Qiu J.: Thawing permafrost reduces river runoff, Nature, doi:10.1038/nature.2012.9749, 2012.

Rawlins M., Lammers R., Frolking S., Fekete B. and Vorosmarty C.: Simulating pan-Arctic runoff with a macro-scale terrestrial water balance model, Hydrol. Process., 17, 2521-2539, doi: 10.1002/hyp.1271, 2003.

Rawlins, M.A., D.J. Nicolsky, K.C. McDonald, and V.E. Romanovsky: Simulating soil freeze/thaw dynamics with an improved pan-Arctic water balance model, J. Adv. Model. Earth Syst., 5:659-675, doi:10.1002/jame.20045, 2013.

Rigon R., Bertoldi G., and Over TM: GEOtop: A distributed hydrological model with coupled water

The Cryosphere Discuss., https://doi.org/10.5194/tc-2017-158
Manuscript under review for journal The Cryosphere
Discussion started: 22 August 2017

and energy budgets, J. Hydrometeorol., 7, 371–388, doi: 10.1175/JHM497.1, 2006.

Schuur, E.A.G., A.D. McGuire, C. Schädel, G. Grosse, J.W. Harden, D.J. Hayes, G. Hugelinus, C.D. Koven, P. Kuhry, D.M. Lawrence, S.M. Natali, D. Olefeldt, V.E. Romanovsky, K. Schaefer, M.R. Turetsky, C.C. Treat, and J.E. Vonk: Climate change and the permafrost carbon feedback, Nature 520,171-179 doi:10.1038/nature14338, 2015.

Sellers, P.J.: Canopy reflectance, photosynthesis, and transpiration, Int. J. Remote Sens., 8, 1335-1372, doi: 10.1080/01431168508948283, 1985.

Sellers, P.J.; Randall, D.A.; Collatz, G.J.; Berry, J.A.; Field, C.B.; Dazlich, D.A.; Zhang, C.; Collelo, G.D.; Bounoua, L.: A Revised Land Surface Parameterization (SiB2) for Atmospheric GCMS. Part I: Model Formulation, J. Clim., 9, 676-705, doi: 10.1175/1520-0442(1996)009<0676:ARLSPF>2.0.CO;2, 1996.

Sjöberg, Y., E. Coon, A. B. K. Sannel, R. Pannetier, D. Harp, A. Frampton, S. L. Painter, and S. W. Lyon: Thermal effects of groundwater flow through subarctic fens: A case study based on field observations and numerical modeling, Water Resour. Res., 52, 1591-1606, doi:10.1002/2015WR017571, 2016.

Song X., Brus DJ, Liu F., Li D., Zhao Y., Yang J. and Zhang G.: Mapping soil organic carbon content by geographically weighted regression: A case study in the Heihe River Basin, China, Geoderma, 261,11–22, doi: 10.1016/j.geoderma.2015.06.024, 2016.

Strahler A N: Quantitative analysis of watershed geomorphology, Eos, Transactions American Geophysical Union, 38(6), 913-920, doi: 10.1029/TR038i006p00913, 1957.

Subin Z.M., Koven C.D., Riley W.J., Torn M.S., Lawrence D.M. and Swenson S.C.: Effects of Soil Moisture on the Responses of Soil Temperatures to Climate Change in Cold Regions, J. Clim.,

The Cryosphere Discuss., https://doi.org/10.5194/tc-2017-158
Manuscript under review for journal The Cryosphere
Discussion started: 22 August 2017

26,3139-3158, doi: 10.1175/JCLI-D-12-00305.1, 2013.

Toon, O.B., McKay, C.P., Ackerman, T.P., and Santhanam, K.: Rapid calculation of radiative heating rates and photodissociation rates in inhomogeneous multiple scattering atmospheres, J. Geophys. Res. 94(D13), 16,287-16,301, doi: 10.1029/JD094iD13p16287, 1989.

Walter W. Immerzeel, Ludovicus P. H. van Beek, and Marc F. P. Bierkens.: Climate Change Will Affect the Asian Water Towers, Science, 328, 1382-1385, doi: 10.1126/science.1183188, 2010.

Walvoord, M. A. and B. L. Kurylyk: Hydrologic Impacts of Thawing Permafrost—A Review, Vadose Zone J., doi:10.2136/vzj2016.01.0010, 2016.

Walvoord, M. A., and R. G. Striegl: Increased groundwater to stream discharge from permafrost thawing in the Yukon River basin: Potential impacts on lateral export of carbon and nitrogen, Geophys. Res. Lett., 34, L12402, doi:10.1029/2007GL030216, 2007.

Wang, L., Koike, T., Yang, K., Jin, R., Li, H.: Frozen soil parameterization in a distributed biosphere hydrological model, Hydrol. Earth Syst. Sc., 14(3), 557-571, doi: 10.5194/hess-14-557-2010, 2010.

Wang Q., Zhang T., Wu J., et al.: Investigation of permafrost distribution over the upper reaches of the Heihe River in the Qilian Mountains, Journal of Glaciology and Geocryology, 35(1), 19-29, 2013 (in Chineses).

Wang Q., Zhang T., Peng X., Cao B., and Wu Q.: Changes of soil thermal regimes in the Heihe River Basin over Western China, Arct., Antarct., and Alpine Res., 47(2), 231-241, doi: 10.1657/AAAR00C-14-012, 2015a.

Wang, Y., Yang, D., Lei, H. and Yang, H.: Impact of cryosphere hydrological processes on the river runoff in the upper reaches of Heihe River, J. Hydraul. Eng., 46, 1064-1071, 2015b (In Chinese).

Wang, Y., Yang, H., Yang, D., Qin Y., Gao B. and Cong ZT.: Spatial interpolation of daily precipitation

The Cryosphere Discuss., https://doi.org/10.5194/tc-2017-158
Manuscript under review for journal The Cryosphere
Discussion started: 22 August 2017

The Cryosphere Discussions

in a high mountainous watershed based on gauge observations and a regional climate model simulation, J. Hydrometeorol.,18, 845-862, 2017, doi: 10.1175/JHM-D-16-0089.1.

Woo, M.-K., Kane, D. L., Carey, S. K. and Yang, D.: Progress in permafrost hydrology in the new millennium, Permafrost Periglac. Process., 19, 237-254, doi:10.1002/ppp.613, 2008.

Woo M K.: Permafrost Hydrology, Springer-Verlag, Berlin Heidelberg, 2012.

Wu, B.F., Yan, N.N., Xiong, J., Bastiaanssen, W., Zhu, W.W., Stein, A.: Validation of ETWatch using field measurements at diverse landscapes: A case study in Hai Basin of China. J. Hydrol., 436, 67-80, doi: 10.1016/j.jhydrol.2012.02.043, 2012.

Wu, B.F.: Monthly Evapotranspiration Datasets (2000–2012) with 1 km Spatial Resolution over the Heihe River Basin, Heihe Plan Science Data Center at Lanzhou, China, doi: 10.3972/heihe.115.2013.db, 2013.

Wu, M., Jansson P. E., Tan X., Wu J., and Huang, J.: Constraining parameter uncertainty in simulations of water and heat dynamics in seasonally frozen soil using limited observed data, Water, 8(2), 64, doi:10.3390/w8020064, 2016.

Wu, Q., and Zhang T.: Changes in active layer thickness over the Qinghai-Tibetan Plateau from 1995 to 2007, J. Geophys. Res., 115, D09107, doi: 10.1029/2009JD012974, 2010.

Yang, D.W., Gao, B., Jiao, Y., Lei, H.M., Zhang, Y.L., Yang, H.B., Cong, Z.T.: A distributed scheme developed for eco-hydrological modeling in the upper Heihe River, China Earth Sci., 58(1), 36-45, doi: 10.1007/s11430-014-5029-7, 2015.

Yang, D.W., Herath, S., and Musiake, K.: Development of a geomorphology-based hydrological model for large catchments, Annu. J. Hydraul. Eng., 42, 169-174, doi: 10.2208/prohe.42.169, 1998.

Yang, D.W., Herath, S., and Musiake, K.: A hillslope-based hydrological model using catchment area and width functions, Hydrol. Sci. J., 47, 49-65, doi: 10.1080/02626660209492907, 2002.

Yang, M., F. E. Nelson, N. I. Shiklomanov, D. Guo, and G. Wan, Permafrost degradation and its environmental effects on the Tibetan Plateau: A review of recent research, Earth Sci. Rev., 103, 31-44, doi: 10.1016/j.earscirev.2010.07.002, 2010.

Ye, B., D. Yang, Z. Zhang, and D. L. Kane: Variation of hydrological regime with permafrost coverage over Lena Basin in Siberia, J. Geophys. Res., 114, D07102, doi:10.1029/2008JD010537, 2009.

Zhao, L., C. L. Ping, D. Q. Yang, G. D. Cheng, Y. J. Ding, and S. Y. Liu: Changes of climate and seasonally frozen ground over the past 30 years in Qinghai-Xizang (Tibetan) Plateau, China, Global Planet. Change, 43, 19-31, doi: 10.1016/j.gloplacha.2004.02.003, 2004.

Zhang, Y.L., Cheng, G.D., Li, X., Han, X.J., Wang, L., Li, H.Y., Chang, X.L., Flerchinger, G.N.: Coupling of a simultaneous heat and water model with a distributed hydrological model and evaluation of the combined model in a cold region watershed, Hydrol. Process., 27(25), 3762-3776, doi: 10.1002/hyp.9514, 2013.

Zhang, Y., Ohata, T., and Kadota, T.: Land-surface hydrological processes in the permafrost region of the eastern Tibetan Plateau, J. Hydrol., 283, 41-56, doi: 10.1016/S0022-1694(03)00240-3, 2003.

Zhou, J.H. and Zheng, Y.R.: Vegetation Map of the upper Heihe basin, Version 2.0, Heihe Plan Science Data Center at Lanzhou, China, doi:10.3972/heihe.426.2014.db, 2014.

The Cryosphere Discuss., https://doi.org/10.5194/tc-2017-158
Manuscript under review for journal The Cryosphere
Discussion started: 22 August 2017

Figure caption:

Figure 1. The Study area, hydrological stations, borehole observation and flux tower stations

Figure 2. Model structure and vertical discretization of soil column

Figure 3. Comparison of the simulated and the observed soil temperature at borehole observation sites, and the observed data is provided by Wang et al. (2013)

Figure 4. Daily soil temperature at the Qilian station: (a) observation; (b) simulation; (c) Simulation-Observation

Figure 5. Comparison of the simulated and observed daily frozen depths during the period of 2002-2014 at: (a) the Qilian station, (b) the Yeniugou station

Figure 6. Comparison of the simulated and the observed hourly liquid soil moisture at the A'rou Sunny Slope station

Figure 7. Comparison of the simulated and the observed daily river discharge at: (a) the Yingluoxia Gauge, (b) the Qilian Gauge, and (c) the Zhamashike Gauge.

Figure 8. Comparison of the simulated and the remote sensing estimated actual evapotranspiration provided by Wu (2013) in the period of 2002~2012

Figure 9. Changes of the mean soil temperature in different seasons: (a) the freezing season (from November to March) (b) the thawing season (from April to October)

Figure 10. Change of the frozen soils in the upper Heihe basin: (a) areas of permafrost and basin averaged annual air temperature; (b) the basin averaged annual maximum frozen depth of the seasonally frozen ground and the annual maximum thaw depth of the permafrost

Figure 11. Distribution of permafrost and seasonally frozen ground: (a) distribution in the period of 1971-1980; (b) distribution in the period of 2001-2010; (c) Areas where where permafrost changed

The Cryosphere Discuss., https://doi.org/10.5194/tc-2017-158
Manuscript under review for journal The Cryosphere
Discussion started: 22 August 2017

into seasonally frozen ground (d) percentage of areas of permafrost and seasonally frozen ground on sunny slope; (e) percentage of areas of permafrost and seasonally frozen ground on shaded slope (the same legend as (d))

Figure 12. Spatial averaged monthly soil temperature during the period of 1971-2013 in different elevation intervals: (a) the seasonally frozen ground with elevation between 3300-3500 m; (b) the areas where permafrost changed to seasonally frozen ground with elevation between 3500-3700 m

Figure 13. Changes of the runoff and actual evapotranspiration: (a) in the freezing season; (b) in the thawing season

Figure 14. Changes of the annual water storage (equivalent water depth) during the period of 1971-2013: (a) the liquid soil water storage of the top 0-3 m layer; (b) the ice water storage of the top 0-3 m layer; (c) the groundwater storage

Figure 15. Model simulated changes of runoff: (a) in the freezing season, (b) in the thawing season

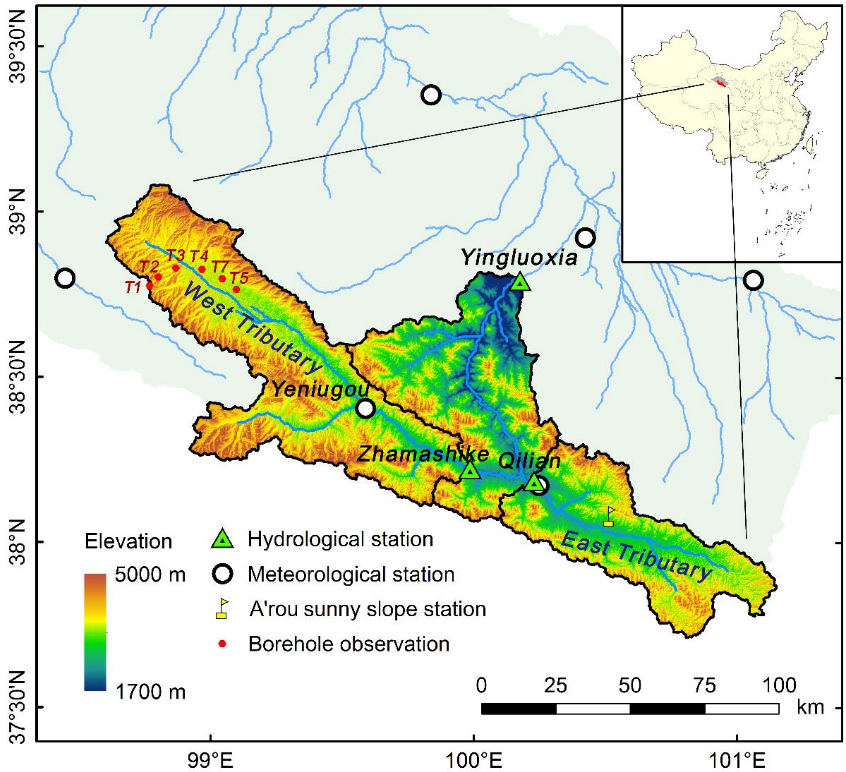

847

848 Figure 1. The Study area, hydrological stations, borehole observation and flux tower

849 stations

850

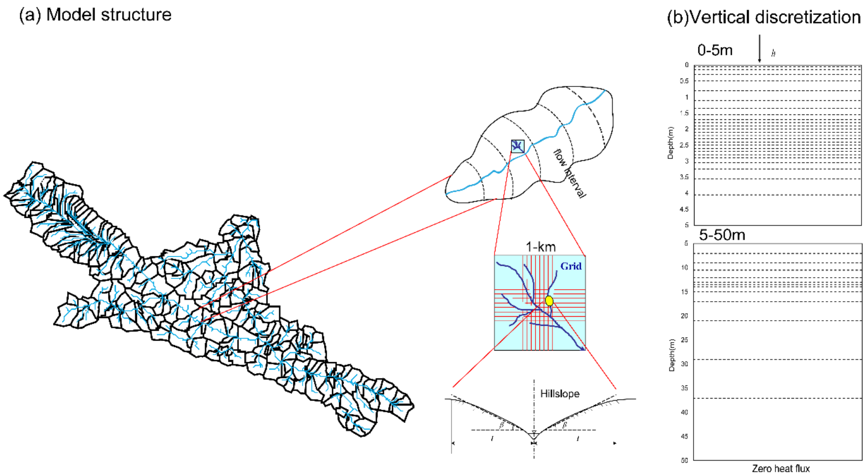

Figure 2. Model structure and vertical discretization of soil column

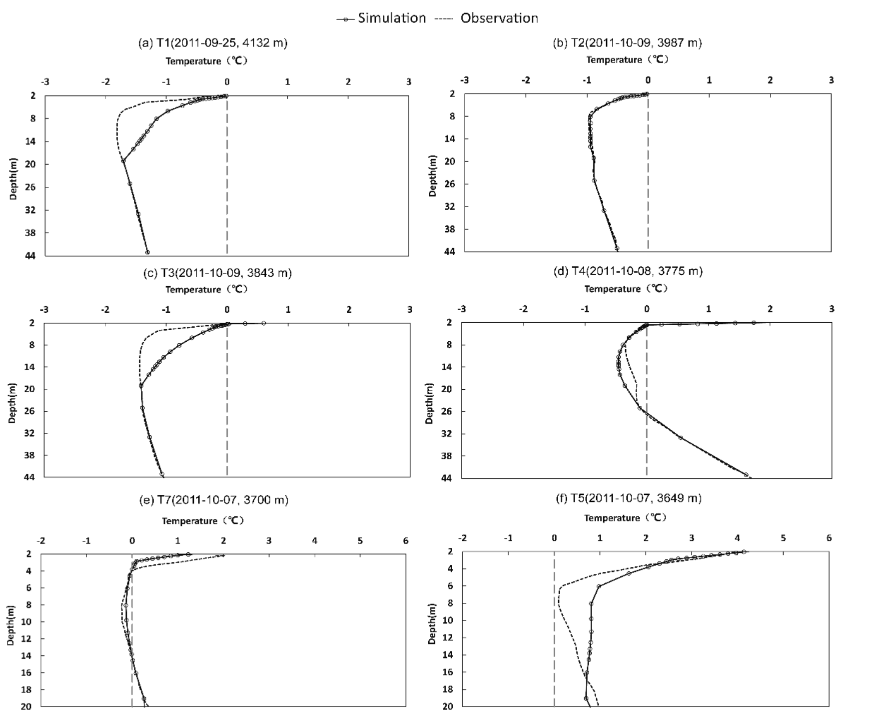

Figure 3. Comparison of the simulated and the observed soil temperature at borehole

The Cryosphere Discuss., https://doi.org/10.5194/tc-2017-158
Manuscript under review for journal The Cryosphere
Discussion started: 22 August 2017

observation sites, and the observed data is provided by Wang et al. (2013)

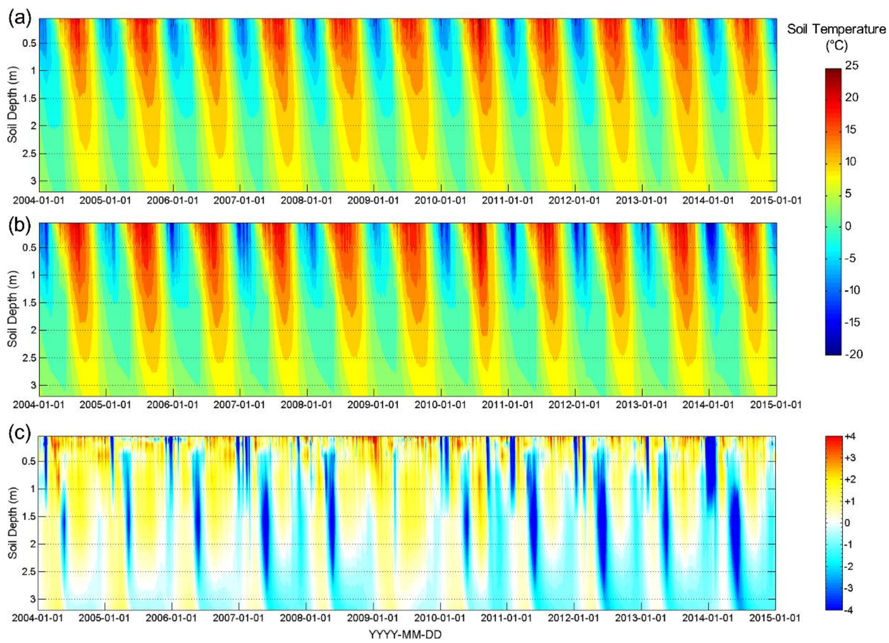

Figure 4 Daily soil temperature at the Qilian station: (a) observation; (b) simulation; (c) Simulation-Observation

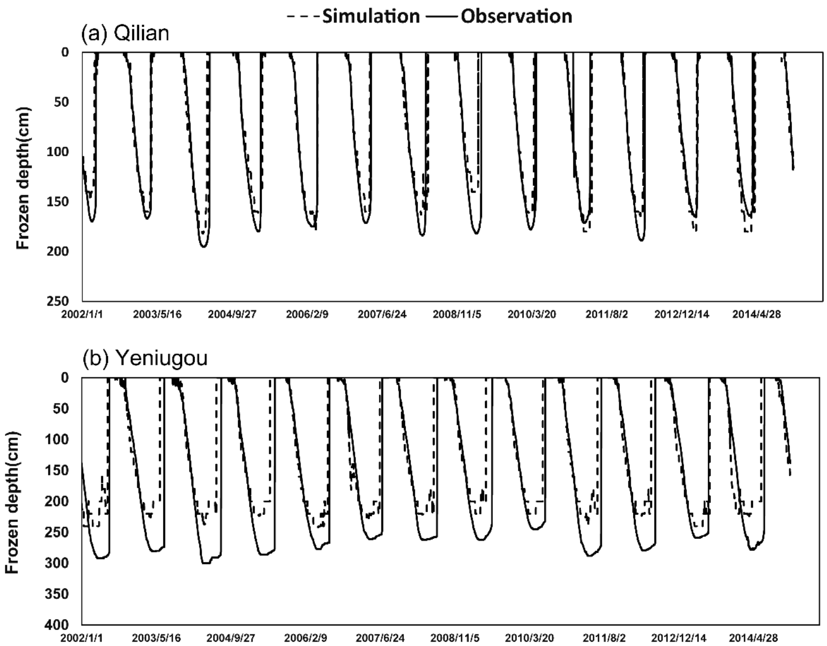

Figure 5. Comparison of the simulated and observed daily frozen depths during the period of 2002-2014 at: (a) the Qilian station, (b) the Yeniugou station

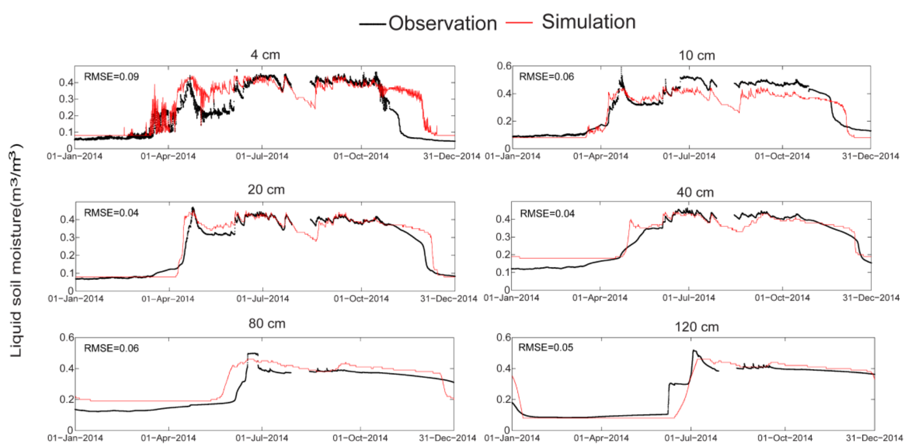

Figure 6. Comparison of the simulated and the observed hourly liquid soil moisture at the A'rou Sunny Slope station

The Cryosphere Discuss., https://doi.org/10.5194/tc-2017-158
Manuscript under review for journal The Cryosphere
Discussion started: 22 August 2017

The Cryosphere Discussions
Open Access
EGU

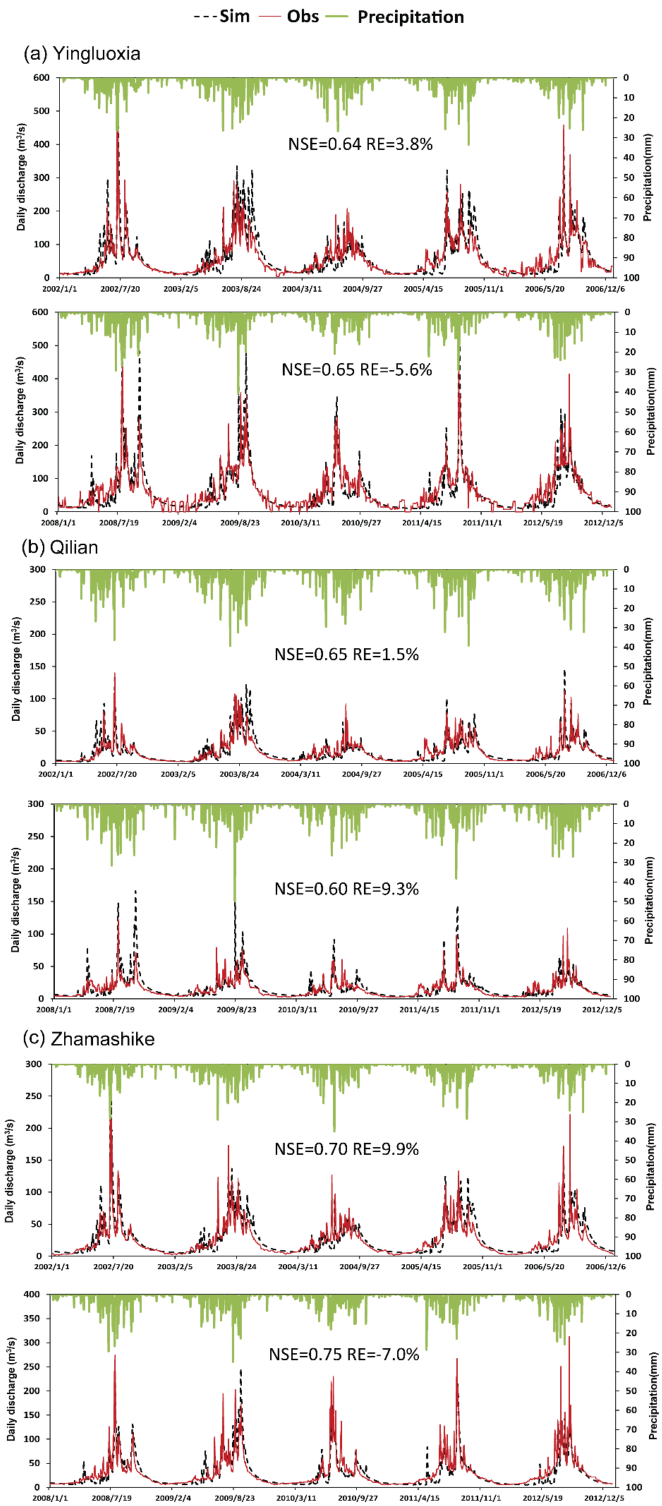

Figure 7. Comparison of the simulated and the observed daily river discharge at: (a) the Yingluoxia Gauge, (b) the Qilian Gauge, and (c) the Zhamashike Gauge.

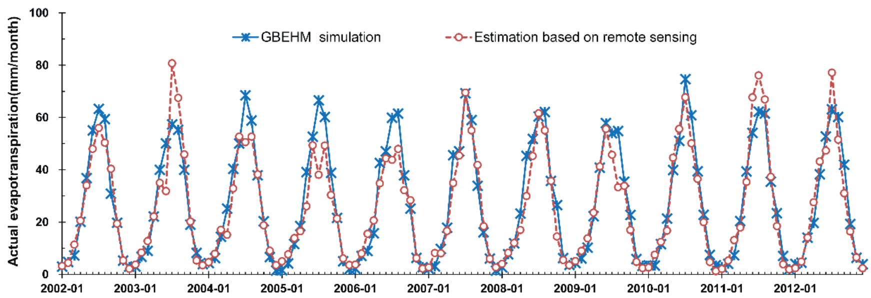

Figure 8. Comparison of the simulated and the remote sensing estimated actual evapotranspiration provided by Wu (2013) in the period of 2002~2012

The Cryosphere Discuss., https://doi.org/10.5194/tc-2017-158
Manuscript under review for journal The Cryosphere
Discussion started: 22 August 2017

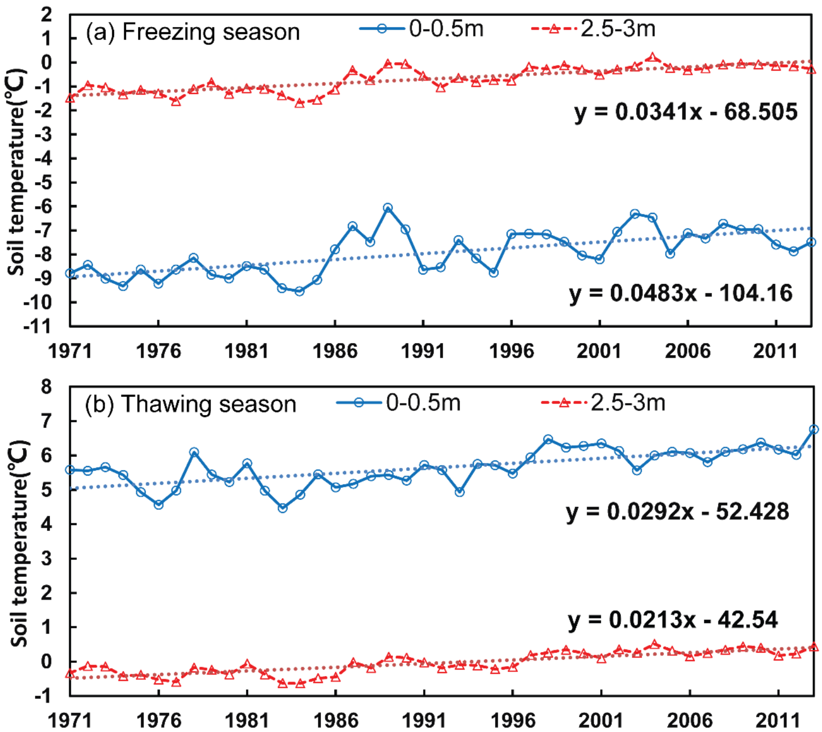

Figure 9. Changes of the mean soil temperature in different seasons: (a) the freezing season (from November to March) (b) the thawing season (from April to October)

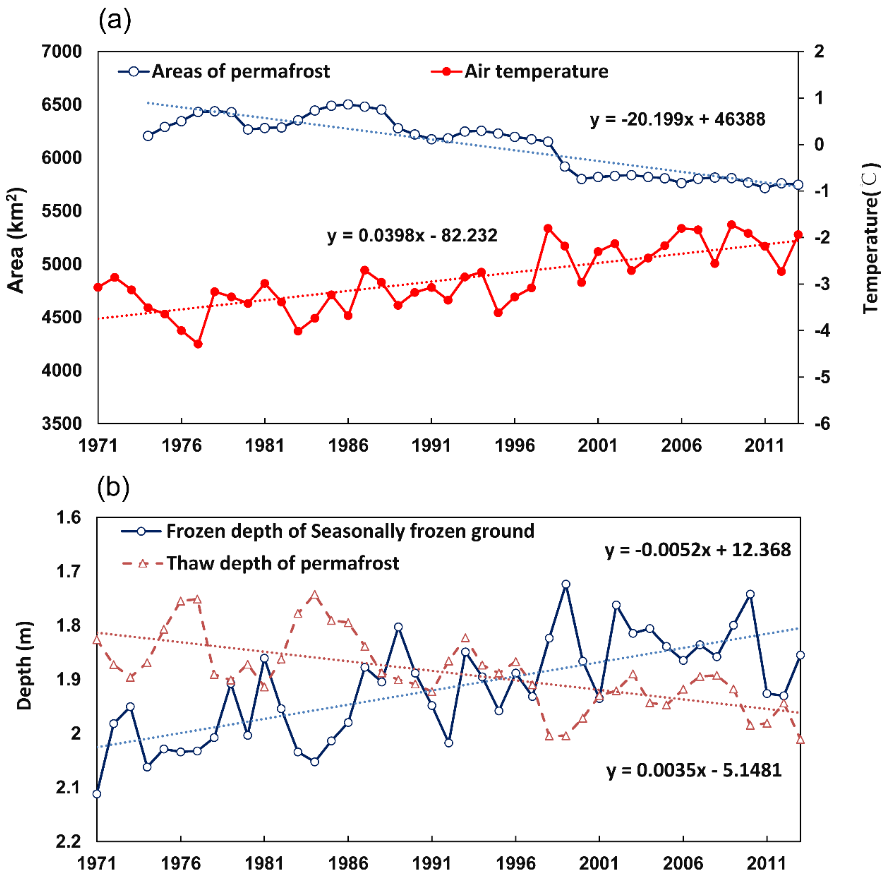

Figure 10. Change of the frozen soils in the upper Heihe basin: (a) areas of permafrost and basin averaged annual air temperature; (b) the basin averaged annual maximum frozen depth of the seasonally frozen ground and the annual maximum thaw depth of the permafrost

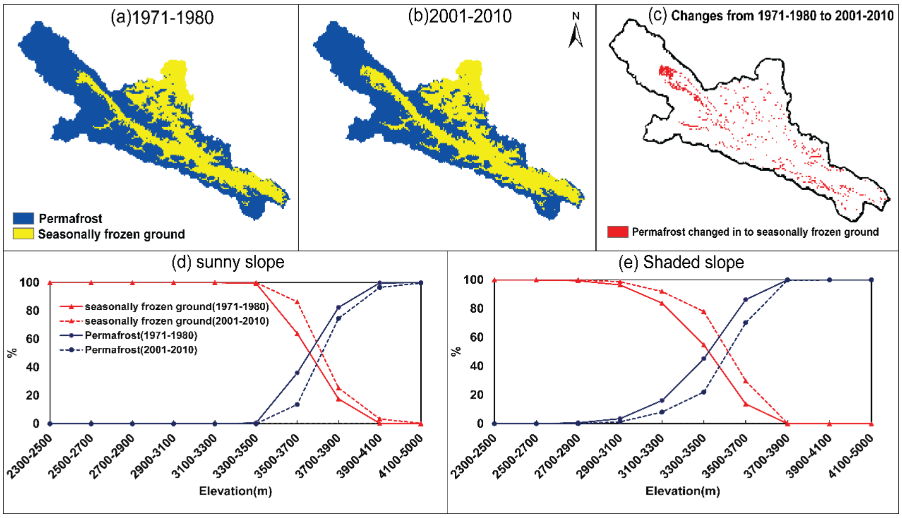

Figure 11. Distribution of permafrost and seasonally frozen ground: (a) distribution in the period of 1971-1980; (b) distribution in the period of 2001-2010; (c) Areas where where permafrost changed into seasonally frozen ground (d) percentage of areas of permafrost and seasonally frozen ground on sunny slope; (e) percentage of areas of permafrost and seasonally frozen ground on shaded slope (the same legend as (d))

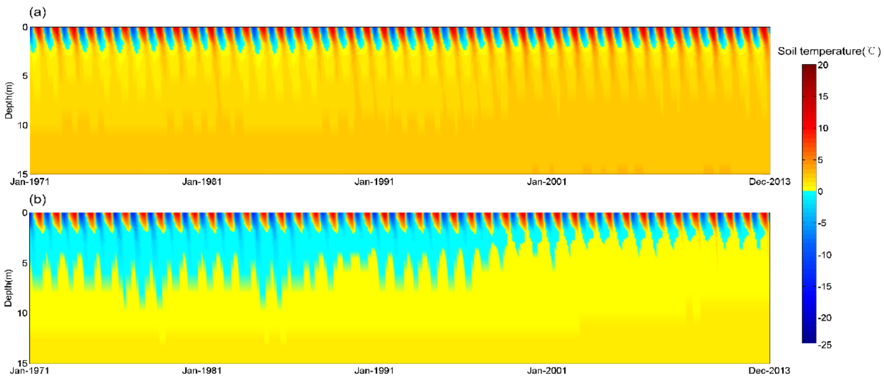

Figure 12. Spatial averaged monthly soil temperature during the period of 1971-2013 in different elevation intervals: (a) the seasonally frozen ground with elevation between 3300-3500 m; (b) the areas where permafrost changed to seasonally frozen ground with elevation between 3500-3700 m

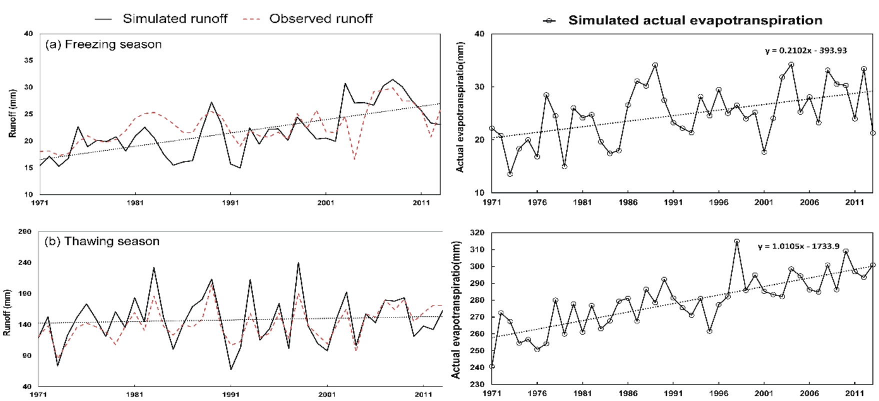

Figure 13. Changes of the runoff and actual evapotranspiration: (a) in the freezing season; (b) in the thawing season

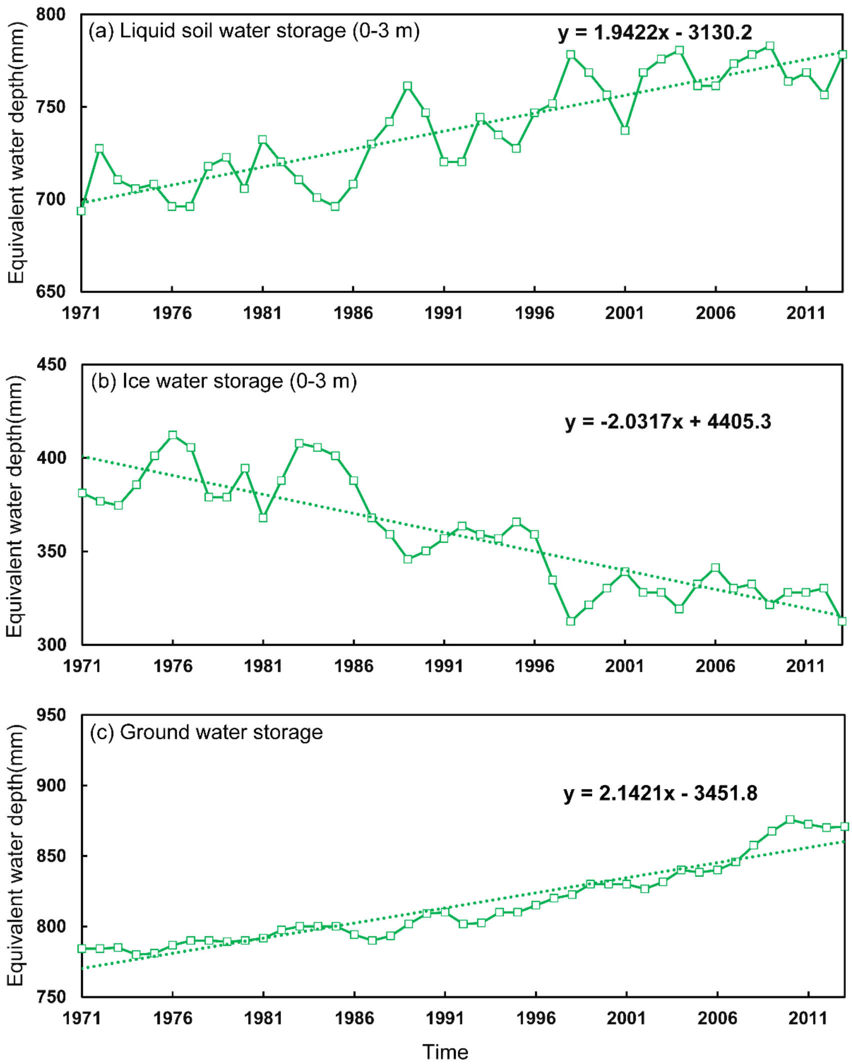

914

915 Figure 14. Changes of the annual water storage (equivalent water depth) during the

916 period of 1971-2013: (a) the liquid soil water storage of the top 0-3 m layer; (b) the ice

917 water storage of the top 0-3 m layer; (c) the groundwater storage

918

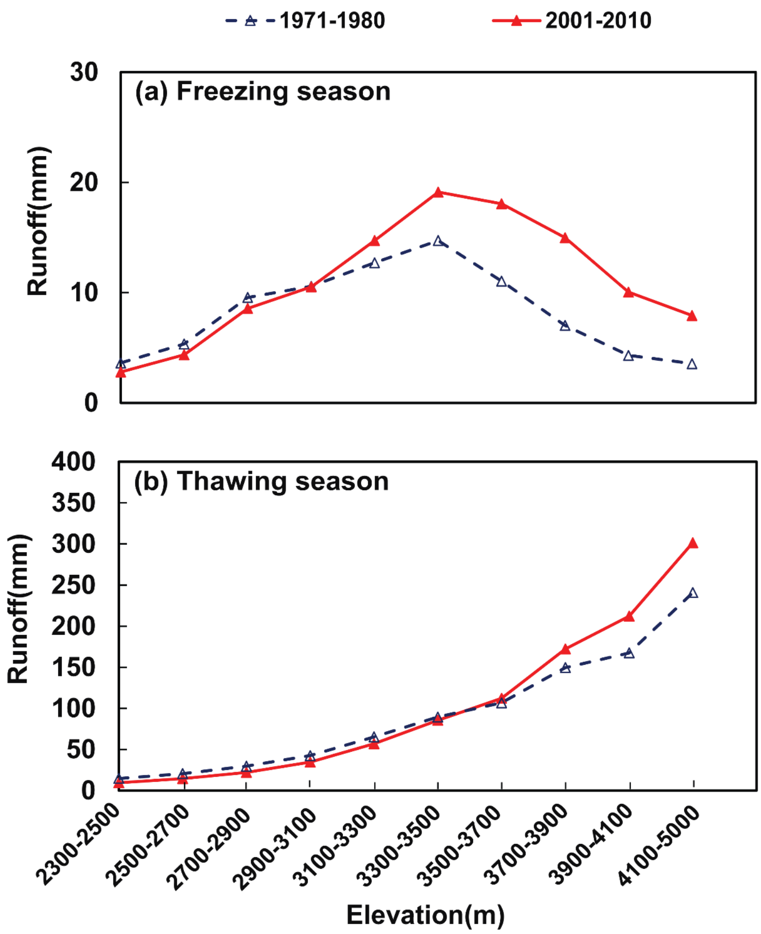

Figure 15. Model simulated changes of runoff: (a) in the freezing season, (b) in the thawing season

The Cryosphere Discuss., https://doi.org/10.5194/tc-2017-158
Manuscript under review for journal The Cryosphere
Discussion started: 22 August 2017

Table list:

The Cryosphere Discuss., https://doi.org/10.5194/tc-2017-158
Manuscript under review for journal The Cryosphere
Discussion started: 22 August 2017

The Cryosphere
Discussions
Open Access
EGU

Table 1 Major parameters of the GBEHM model

Parameters	Coniferous Forest	Shrub	Steppe	Alpine Meadow	Alpine Sparse Vegetation	Desert
Surface retention capacity (mm)	30.0	25.0	10.0	15.0	15.0	5.0
Surface roughness (Manning coefficient)	0.5	0.3	0.1	0.1	0.1	1.0
Soil reflectance to visible light	0.20	0.20	0.20	0.28	0.14	0.11
Soil reflectance to near-infrared radiation	0.225	0.225	0.225	0.28	0.225	0.225
Leaf reflectance to visible light	0.105	0.105	0.105	0.105	0.105	—
Leaf reflectance to near-infrared radiation	0.35	0.58	0.58	0.58	0.58	—
Leaf transmittance to visible light	0.05	0.07	0.07	0.07	0.07	—
Leaf transmittance to near-infrared radiation	0.10	0.25	0.25	0.25	0.25	—
Maximum Rubsico capacity of top leaf (10^{-5} mol·m^{-2}·s^{-1})	6.0	6.0	3.3	3.3	3.0	—
Plant root depth (m)	2.0	1.0	0.40	0.40	0.1	0.0
Intrinsic quantum efficiency (mol·mol^{-1})	0.08	0.08	0.05	0.05	0.05	—
Canopy top height (m)	9.0	1.9	0.3	0.3	0.2	—
Leaf length (m)	0.055	0.055	0.3	0.3	0.04	—
Leaf width (m)	0.001	0.001	0.005	0.005	0.001	—
Stem area index	0.08	0.08	0.05	0.05	0.08	—

Table 2 Changes in annual basin water balance and runoff components in different seasons

Decade	Precipitation (mm/yr)	Actual evaporation (mm/yr)	Simulated runoff (mm/yr)	Observed runoff (mm/yr)	Runoff ratio(observed)	Runoff ratio (simulated)	Runoff components (mm/yr)					
							Freezing season (from November to March)			Thawing season(from April to October)		
							T	G	S	T	G	S
1971-1980	439.1	280.8	154.5	143.8	0.33	0.35	18.5	0.0	0.0	136.0	3.5	13.5
1981-1990	492.8	300.0	186.2	174.1	0.35	0.38	20.2	0.0	0.0	166.1	3.1	28.2
1991-2000	471.0	306.1	160.1	157.4	0.33	0.34	20.4	0.0	0.0	139.7	3.8	19.2
2001-2010	504.3	317.4	177.9	174.3	0.35	0.35	27.2	0.0	0.0	150.7	3.7	25.8

Note: T means total runoff, G means glacier runoff and S means snowmelt runoff.